

# A structural study of the myristoylated N-terminus of ARF1

Thad A. Harroun<sup>a,\*</sup>, Jeremy P. Bradshaw<sup>b</sup>, Kia Balali-Mood<sup>b</sup>, John Katsaras<sup>a</sup>

<sup>a</sup>National Research Council, Neutron Program for Materials Research, Chalk River Laboratories, Chalk River, ON, Canada K0J 1J0

<sup>b</sup>Preclinical Veterinary Sciences, University of Edinburgh, Summerhall, Edinburgh EH8 1QH, UK

Received 7 October 2004; received in revised form 1 December 2004; accepted 2 December 2004

Available online 18 December 2004

## Abstract

The effect of myristoylation on the 15-amino-acid peptide from the membrane-binding N-terminus of ADP ribosylation factor 1 (ARF1) was studied using neutron diffraction and circular dichroism. A previous study on the non-acylated form indicated that the peptide lies parallel to the membrane, at a shallow depth and in the vicinity of the phosphorylcholine headgroups. It was suggested that the helix does not extend past residue 12, an important consequence for the linking region of the ARF1 protein. In this paper, we show that the result of myristoylation is to increase the helical content reaching the peptide's C-terminus, resulting in the formation of a new hydrophobic face. This increased helicity may augment the entire protein's membrane-binding affinity, indicating that ARF1 effectively has two interdependent membrane-binding motifs.

© 2004 Elsevier B.V. All rights reserved.

**Keywords:** ADP ribosylation factor (ARF); Phospholipid; Neutron diffraction; Myristoylation

## 1. Introduction

Myristoylation is a common post-transcriptional modification of proteins that involves the covalent attachment of a saturated, fourteen-carbon fatty acid to the N-terminal glycine. Such a modification confers additional membrane-binding affinity through the lipid anchoring properties of the myristoyl chain. The utility of myristoylation is as varied as the functions of the numerous proteins that are modified in this way [1].

Adenosine diphosphate ribosylation factors (ARF) are just one type of myristoylated proteins. ARFs are a family of GTP-binding proteins, abundant and ubiquitous in eukaryotic cells. Their strongest characteristic is their regulatory behavior on different forms of membrane fusion, including vesicle formation, secretion, and endocytosis.

ARF1, in particular, is involved in the regulation of vesicle transport in the Golgi apparatus [2–5] and the

activation of phospholipase D (PLD) in the process of secretion of granules from neutrophil-like cells [6]. In the inactive state, ARF1 is bound to GDP and is found soluble in the cytosol. ARF1 switches to its active form upon interaction with any number of guanine exchange factors (GEFs), with a conserved Sec7 domain [7]. ARF1 exchanges its GDP for GTP, the myristoyl chain is unfurled, and the protein binds to the Golgi membrane [8]. From there, it serves as a necessary cofactor for the regulation of the proteins involved in the packaging and coating of coat protein complex I (COPI) vesicles [9]. After the transport of the vesicle, ARF1 hydrolyses GTP under the influence of GTPase Activation Protein (GAP) and releases from the membrane, reverting back to its inactive state.

The role of the myristoyl chain in this case is not clear. Data suggests that there are two contributors to ARF1's ability to bind to membranes: the myristoyl chain and the N-terminus helix. Membrane-binding persists upon the removal of the acyl chain [10], and secretory function is restored upon the addition of non-Myr-ARF1 to ARF1 depleted cells [11]. However, ARF1 activity is considerably altered upon the removal of the N-terminus [12]. Mutant

\* Corresponding author. Tel.: +1 613 584 8811x6237; fax: +1 613 584 4040.

E-mail address: [Thad.Harroun@nrc.gc.ca](mailto:Thad.Harroun@nrc.gc.ca) (T.A. Harroun).

ARF1 with 17 residues deleted from the N-terminus no longer activates PLD and inhibits coat protein recruitment in competition with the wild type ARF1 [13]. This is despite the fact that ARF1 can still bind to GTP strongly without its N-terminus.

There have been crystal structures of the non-myristoylated, inactive form of ARF1 [2] and one structure of the GTP bound form, with the 17 N-terminus amino acids deleted [14]. (For a review of ARF crystal structures, see Ref. [15]). However, not enough is known about the membrane bound structure [16]. It is thus important to determine how ARF1 acts to bring together the necessary proteins in COPI vesicle formation.

We have previously determined the location and orientation of the non-acylated form of the fifteen-amino-acid peptide from the N-terminus of human ARF1 (ARF1p) [17]. Our conclusions from that study, and subsequent analysis by molecular dynamics simulations [18,19], were that the peptide lies parallel to the plane of the membrane, among the lipid headgroups. At that time, we suggested that the amount of helix in the peptide did not extend much past Phe12. The structural characterization in that analysis was already further than any reported to date, as it was based on the determination of total secondary structure and the location in the bilayer of three labeled residues. Two recent NMR studies have attempted a similar determination of the myristoylated form of ARF1p N-terminus segment (Myr-ARF1p) in a lipid environment [20,21]. However, the efficacy of this method is somewhat questionable, because the structure was based on no more than the orientation of three individual peptide bonds with respect to the plane of the membrane. The locations in the membrane of groups or bonds were not determined, however, the conclusions regarding peptide orientation and location were similar to Davies et al. [17].

In this paper, we extend our first experiments, this time concentrating on the role that myristoylation plays on the membrane-binding properties of Myr-ARF1p. We find that the addition of the myristoyl chain increases the helical content of the peptide, resulting in a new hydrophobic face for membrane binding. This data may have important implications for explaining the previous membrane-binding data.

## 2. Methods

The technique of neutron lamellar diffraction with specific deuterium labeling is based on the method of Weiner and White [22] and extended by Bradshaw et al. [23]. In summary, the technique involves the one-dimensional reconstruction of the bilayer profile, normal to the plane of the membrane, using common methods of crystallography. For neutron diffraction, this results in a map of the neutron scattering length of the bilayer cross section, rather than the electron density measured by X-ray

crystallography. The result is a low-resolution, time- and sample-averaged profile of the bilayer. One can then utilize the significant difference between hydrogen and deuterium in their ability to scatter neutrons, to label specific parts of the system. The difference between the scattering length density profiles of the H and D samples yields a higher resolution, time- and sample-averaged map of the location of the label.

The techniques employed here do not differ significantly from the previous experiment with the non-myristoylated ARF1p. Four versions of the Myr-ARF1p peptide were synthesised (Dalton Chemical Laboratories, Toronto, Canada): one in its normal hydrogenated form, and three with single amino acid labeling. Deuterium labeling involved replacing the five hydrogen atoms around the phenylalanine ring with deuterium, each in turn at the Phe4, Phe8, and Phe12 residue positions. Peptides were incorporated into bilayers composed of DOPC:DOPG 7:3 at 3 mol% by co-dissolving in chloroform:trifluoroethanol 1:1 and spraying onto a silicon slide with an artist's airbrush. This results in multilayer stacks of highly aligned bilayers.

Data were collected on the N5 spectrometer located at the Chalk River Laboratories, Canada. Typically five orders of diffraction were collected at hydrations ranging from 84% RH to 97% RH, and D<sub>2</sub>O concentrations ranging from 8–80%. The samples were kept at a temperature of  $30.0 \pm 0.5$  °C with a circulating water bath. Sample equilibration was determined after sequential  $\theta$ – $2\theta$  scans, which showed no change in the position of the Bragg peaks. For better statistics, several data sets were averaged. Bragg peaks were fitted with Gaussian functions, and the integrated peak intensity, less the background, was taken as the measured structure factor. After correcting the data for sample geometry and absorption, the structure factors for all three labels were scaled and subtracted simultaneously. Gaussians were fit, in reciprocal space, to the difference between the labelled and unlabelled structure factors to determine the label positions, with a typical chi-squared value of 0.01.

CD samples were made by dissolving Myr-ARF1p in either a buffer, pH 7.4, of 10 mM Tris and 0.1 mM EDTA or a solution of TFE, at concentrations of 2 mg/ml. Data were taken on a Jasco J600 spectropolarimeter at the NRC's Institute for Biological Sciences, Canada. Data were averaged and background corrected. The spectra were fit with the program CDPro to determine the helical content.

## 3. Results and discussion

The difference in the structure factors between the deuterated and hydrogenated samples under the same conditions can be modeled as a Gaussian shaped peak in real-space, the parameters of which reveal important positional information regarding the label [22]. The first parameter to be determined is the position of the peak,

which is centered at the time-averaged center-of-mass of the phenylalanine ring (specifically its hydrogens), as measured from the center of the bilayer. The second parameter is the width of the peak, which indicates the time-averaged fluctuation amplitude of the phenylalanine ring, averaged over all of the peptides in the sample. Finally, the amplitude of the peak is simply the scattering length density of 5 deuteriums less that of 5 hydrogens. This last piece of information is used to properly scale the data.

Fig. 1 shows the positions (dotted line) of the three different labeled residues. Each label is well described by a single Gaussian (solid line), and all three labels clearly occupy only one position, situated about 16 to 18 Å from the bilayer center. The small undulations in the data stem from small errors in the structure factors and the subsequent Fourier reconstruction. Such ripples are encountered in all reconstructions of electron density or neutron scattering length, but are more pronounced in this case since we only have a few orders in the Fourier series (Fourier termination errors) when compared with a typical case in protein crystallography [24], where the system is overdetermined. The data was scaled according to the area under the peaks, a method that is self-consistent by whether or not, in the final subtraction, the unlabeled structure factor scales to the same value for each label.

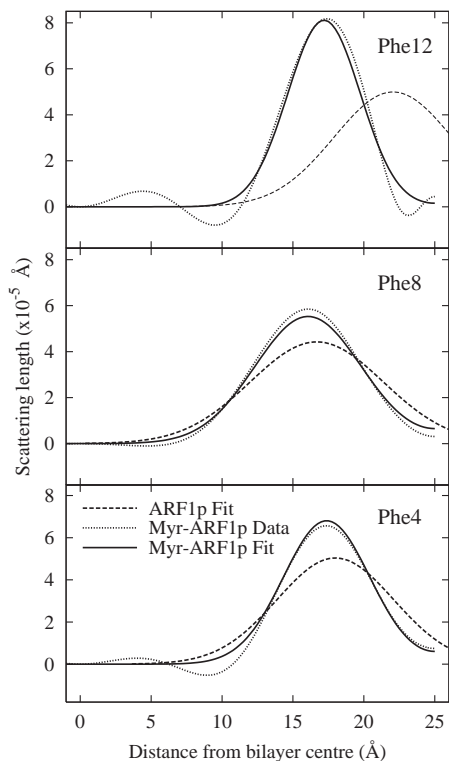


Fig. 1. The location of the deuterium labeled phenylalanines of ARF1p and Myr-ARF1p, determined from neutron diffraction. The abscissa is measured from the center of the DOPC:DOPG (7:3) bilayer, and the ordinate is the measured neutron scattering length per unit length of the label. The solid line is a Gaussian fit to the Myr-ARF1p data, shown as a dotted line. The dashed line represents the previous non-myristoylated ARF1p data for comparison [17].

Table 1

The location and standard deviation widths of the deuterium labels, determined by neutron diffraction

		Phe4	Phe8	Phe12
ARF1p	Position	17.99±0.02	16.68±0.04	22.06±0.06
	S.D.	5.83±0.03	6.64±0.04	5.88±0.08
Myr-ARF1p	Position	17.37±0.02	16.07±0.03	17.20±0.04
	S.D.	4.32±0.07	5.31±0.06	3.62±0.03

The location is measured in angstroms from the center of the bilayer. The data for ARF1p is taken from Davies et al. [17].

Included in Fig. 1, as a dashed line, are the results from the case of the non-myristoylated peptide. For Phe4 and Phe8, there is little difference in the location of the labels. Both residues are clearly in the hydrophobic/hydrophilic interface region of the lipid headgroups. In the Myr-ARF1p case, the fluctuation amplitudes are reduced, indicating that the phenylalanines are in a more constrained configuration and are undergoing somewhat less motion. The locations and standard deviation widths of the Myr-ARF1p peaks are given in Table 1, along with the results from the reference of Davies et al. The greatest difference between the myristoylated and non-acyl peptides is found with Phe12. For ARF1p, Phe12 stands above the headgroup region and fluctuates considerably, whereas with Myr-ARF1p, Phe12 is brought closer into the headgroups and, in comparison, is more immobile than the other measured residues.

By fitting a secondary structure to the data, we can elucidate the significance of the Phe12 difference between the myristoylated and non-acyl peptides. Here, we follow a similar method to that of Davies et al. and use circular dichroism and an atomic structure model to determine the possible modes of peptide interaction with the membrane. At least four deuterated labels would be required in order to orient a peptide secondary structural model unambiguously. One way of approaching this geometrical problem is to consider that it is possible to fit a plane triangle to any three points, but that the two opposing sides of the plane can be interchanged. The result of “flipping” the whole peptide between the two solutions can be quite dramatic to the overall orientation of the peptide relative to the membrane; the two models may be wholly unrelated, despite the fact that both have the same residues at the same depth in the bilayer. Although we are left with two mathematical alternatives, we can usually reject one on energetic and thermodynamic principles.

Before we can construct our model, we must determine its overall secondary structure using circular dichroism. Fig. 2 is the CD spectrum of Myr-ARF1p in buffer and TFE. In both polar and non-polar environments, the peptide adopts a strongly helical structure. This is in sharp contrast to ARF1p, which is predominantly a random-coil in buffer, and only partially self-folds into a helix in TFE or a lipid environment. The observation of helix promotion by myristoylation is not unexpected, such an effect has been reported in a peptide from CAMP-dependent protein kinase,

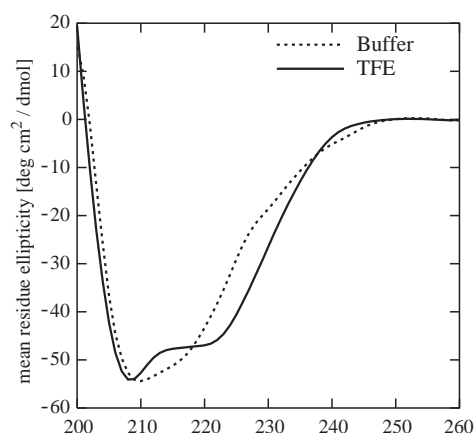


Fig. 2. Circular dichroism of Myr-ARF1p in TFE and aqueous buffer. Under both hydrophilic and hydrophobic environments, the myristoylated peptide adopts a nearly 100%  $\alpha$ -helical structure.

though not to the same extent seen here [5]. The peptide's helical content was determined by CONTIN analysis and shows nearly 100%  $\alpha$ -helix with little or no random coil in TFE. In buffer, the peptide is also predominantly helical, although analysis indicates that of the 80% helical content, as much as 20% of it is  $\beta$ -strand. The data indicates that the peptide possesses nearly complete amount of ordered secondary structure, much greater than indicated by the non-myristoylated crystal structure.

We begin with a starting model taken from a segment of the crystal structure of the full, non-myristoylated ARF1. This model has much less helical content than the CD data indicates, but its inclusion is instructive. We are not concerned with representing the myristoyl chain in the model, since we assume that it is always inserted in the same bilayer that the peptide is associated with. Fig. 3 is a diagram of the peptide, oriented with Phe labels at the positions shown in Fig. 1. In Fig. 3, only the backbone trace is shown, and the long axis of the molecule is viewed end-on. The block slab in the picture is meant to suggest the lipid

bilayer headgroup region, extending between 16 and 20 Å from the center of the bilayer [22]. The water layer is above the slab and the hydrocarbon matrix below. The model sits in the headgroup region, with its long axis parallel to membrane plane. As discussed above, models A and B in Fig. 3 are mathematically optional orientations. Based on thermodynamic reasoning, we suggest that model B is incorrect, since its charged residues such as Lys14 and Lys15 are unexpectedly found buried in the center of the bilayer.

To confirm that these models have opposite hydrophobic/hydrophilic orientations, we calculate the hydrophobic moment of each model. The hydrophobic moment is taken to be the vector joining the hydrophilic and hydrophobic barycenters  $\vec{\mu}$ , calculated using the following relationship

$$\vec{\mu} = \frac{\sum_i H_i \vec{r}_i}{\sum_i H_i},$$

where  $H_i$  is the free energy transfer for each atom between the water and the hydrocarbon chain environments, and  $\vec{r}_i$  is the atomic coordinate [25]. The sum is taken over all hydrophobic or hydrophilic atoms and has the units of Å. In Fig. 3, the hydrophobic moment is drawn as a ball-and-stick, joining the hydrophobic center of mass (in black) with the hydrophilic center of mass (in white). Although neither model has a vertically oriented moment, as one might expect for a ideal amphipathic helix, we see that in model B, the hydrophobic center is closer to the water and farther from the bilayer than the hydrophilic center. Of the two models, model A is therefore the more correct of the two.

The helical content of models A and B is much less than indicated by the CD data, so we created a second model by restricting the  $\Phi/\Psi$  angles of the backbone to form a tighter  $\alpha$ -helix. The model was then subjected to 1000 steps of energy minimization to remove bad steric contacts that might have been created. Fig. 4 shows this new model in both possible orientations. From the figure, we can see that

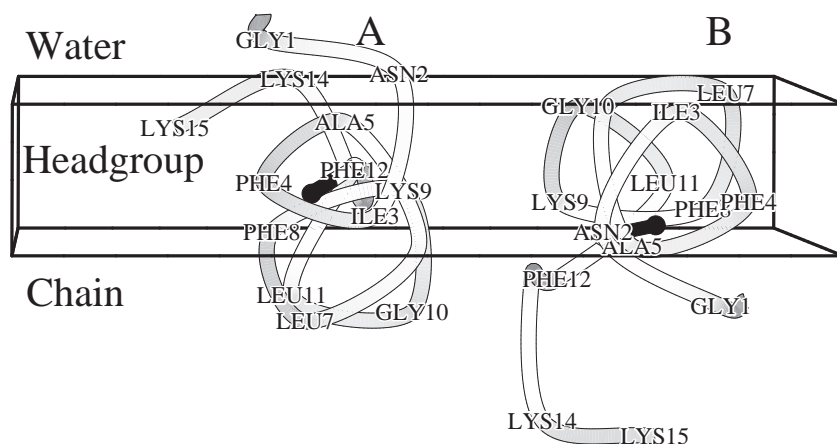


Fig. 3. The orientation of a model of Myr-ARF1p. The secondary structures of these models are derived from the crystal structure of the full ARF1 protein. Models A and B are mathematically related (see text for discussion). The slab indicates the lipid headgroup region extending from 16 to 20 Å from the bilayer center. The shading is only meant to suggest a 3D appearance. Figs. 3–5 were made with Molscript [26].

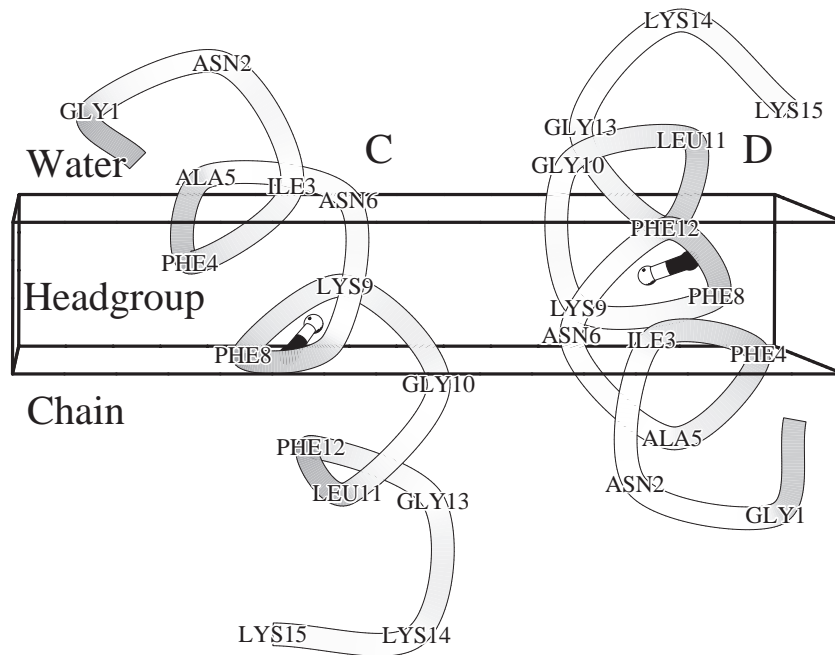


Fig. 4. The orientation of a more helical model of Myr-ARF1p. The secondary structures of these models come from increasing the helical content of models A and B. The shading is only meant to suggest a 3D appearance.

the models are unreasonably tilted out of the plane of the bilayer. The backbone atoms of models C and D were fit with a straight line to define the helical axis, which make  $38^\circ$  and  $26^\circ$  angles to the membrane plane, respectively. The tilt is primarily due to the movement of the Phe12 away from the opposite side of the molecule from Phe4 and Phe8, as seen in model A. In this configuration, Phe12 is at its greatest distance around the molecule from Phe4 and 8, making it very difficult to place all three residues at the same depth in the bilayer (ref. Fig. 1). Phe12 should ideally be on the opposite side to Phe4 and 8, as in model A, or they should all lie on the same side of the peptide.

Model E, shown in Fig. 5, is an ab initio, ideal  $\alpha$ -helix constructed from the peptide sequence. In this arrangement, Phe12 is on the same side as Phe4 and Phe8, forming a new face of the molecule that theoretically should be expected to

lie at the hydrophobic/hydrophilic interface. The peptide in this model again lies parallel to the membrane, although it “rides” higher in the headgroup region than model A. Since all three Phe’s are so close to each other, there is very little difference between model E and its alternative fit (not shown), unlike models A and C. The Lys15 at the C-terminus pointing toward the acyl chain region is somewhat misleading, as the full side chain snorkels up to the polar end of the lipids.

The hydrophobic moments of models C and D are perpendicular to the helical axis, indicating that the tightening of the helix is forming a new hydrophobic face. In model E, the hydrophobic moment is nearly vertical and at its maximum magnitude, as one might expect from an ideal helix with a periodic hydrophobic sequence. The difference in structure between models A and E is minor.

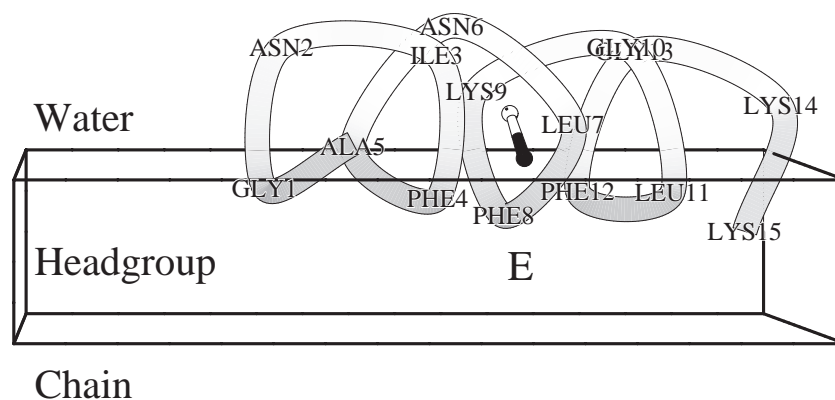


Fig. 5. The orientation of an ab initio model of Myr-ARF1p. In this case, the hydrophobic/hydrophilic centers-of-mass are at their greatest separation and alignment with the hydrophobic gradient normal to the membrane interface, which is expected from a peptide with a periodic hydrophobic sequence.



Model E therefore seems to be the best candidate for membrane associated peptide.

The data presented here show that the effect of myristoylation on ARF1 peptide is greater than previously thought. Taking into consideration our previous data, it seems that the myristoyl chain addition is a requirement for the membrane-binding domain to achieve its maximum ideal secondary structure suitable for membrane binding. The idea that the addition of myristic acid to the N-terminus can have structural effects extending further along the peptide is not unexpected. The PROSITE (PDOC00008) definition of amino acid sequence that is a candidate for modification by myristoyl CoA:protein N-myristoyl transferase (NMT) indicates that the motif extends at least 6 residues from the N-terminus. However, another analysis of a larger set of identified myristoylated proteins suggests that the motif extends as many as 17 amino acids from the N-terminal glycine [1].

The above support our observations of a greatly enhanced helix with myristoylation. Model A is a likely candidate structure for the non-myristoylated protein; considerable helix remains, enough to maintain some membrane-binding affinity as seen in the biochemical studies. Once myristoylated, the amount of helix increases, and with it, the membrane-binding affinity and localization of certain residues at the membrane interface is also increased. Model E is not simply a better-defined helix than model A, it is also rotated along the long axis in the membrane.

ARF1 without its N-terminus can bind GTP but cannot set in motion the process of vesicle formation *in vitro*. Specifically, it no longer activates PLD and interferes with coatamer formation. Although it has been suggested that vesicle secretion may be linked to PLD-dependent, phosphatidic acid production [11], there is indication that the non-Myr-ARF1 competes with Myr-ARF in the process, inhibiting coat formation regardless of PLD activity [13].

The localization of the protein at the membrane interface is important, conceivably to gather together the necessary coat and packaging proteins. Jones et al. identify the two lysines 14 and 15 as necessary for PLD activation, and furthermore, substituting the ARF1 N-terminus on ARF6 greatly enhances overall ARF activity [13]. (Note that residue numbering in our case does not count the Myr as residue 1.) In that paper, the authors draw a picture of a plausible structure of membrane-bound ARF1, in which residues Lys14 and Lys15 are part of the linking domain to the rest of the protein. From inspection, this model is remarkably similar to the non-myristoylated ARF1p model in the location of lysines and phenylalanines made by us. Here, we are suggesting that because of myristoylation, those residues are more a part of the helix, rather than the linking region, and positioned closer to the membrane headgroups. Thus, the role of Myr may be to carry out the final positioning for the activation of the ARF1 protein.

It is hoped that the data presented here will stimulate molecular dynamics simulation studies of similar membrane-binding protein domains. However, experimental data of these systems is required for the proper construction and analysis of such simulations. In this regard, the neutron diffraction data in this report is unique. The data of Fig. 1 is directly comparable to the static and time-averaged structure of a simulation, on a per-residue or per-atom group basis. Unlike other techniques, deuterium labeling does not suffer from the inherent perturbations of large molecular probes and labels. Furthermore, neutron diffraction is a reasonably direct structure determination technique and whose data does not require extensive interpretation, as can be the case with some spectroscopies. The only ambiguity with the data, is in determining which best-fit model is more probable. As we have shown, after vetting the possible protein structures with known information from other experiments one can arrive at a solution. Moreover, the location of the labeled residues, shown in Fig. 1, is accurate and unambiguous.

In conclusion, we have shown that the location of the myristoylated N-terminus of ARF1 lies flat within the headgroup region of the membrane. Using structural data and modeling, we have argued that the effect of the acyl chain modification is to increase the amount of helix in the peptide, resulting in the formation of a new hydrophobic face with increased affinity for the hydrophobic/hydrophilic interface. This implies that the role of myristoylation is to provide ARF1 with two interdependent membrane-binding domains.

## References

- [1] S. Maurer-Stroh, B. Eisenhaber, F. Eisenhaber, N-terminal N-myristoylation of proteins: prediction of substrate proteins from amino acid sequence, *J. Mol. Biol.* 317 (2002) 541–557.
- [2] J.C. Amor, D.H. Harrison, R.A. Kahn, D. Ringe, Structure of the human ADP-ribosylation factor 1 complexed with GDP, *Nature* 372 (6507) (1994) 579–710.
- [3] K.M. Jacques, Z. Nie, S. Stauffer, D.S. Hirsch, L.-X. Chen, K.T. Stanley, P.A. Randazzo, Arf1 dissociates from the clathrin adaptor GGA prior to being inactivated by Arf GTPase-activating proteins, *J. Biol. Chem.* 277 (49) (2002) 47235–47241.
- [4] J. Menetrey, E. Macia, S. Pasqualato, M. Franco, J. Cherfils, Structure of Arf6GDP suggests a basis for guanine nucleotide exchange factors specificity, *Nat. Struct. Biol.* 7 (6) (2000) 466–469.
- [5] A. Tholey, R. Pipkorn, D. Bossemeyer, V.K.J. Reed, Influence of myristoylation, phosphorylation, and deamidation on the structural behavior of the N-terminus of the catalytic subunit of CAMP-dependent protein kinase, *Biochemistry* 40 (2001) 225–231.
- [6] S. Cockcroft, G.M.H. Thomas, A. Fensome, B. Geny, E. Cunningham, I. Gout, I. Hiles, N.F. Totty, O. Troung, J.J. Hsuan, Phospholipase D: a downstream effector of ARF in granulocytes, *Science* 263 (1994) 523–526.
- [7] S. Béraud-Dufour, S. Paris, M. Chabre, B. Antonny, Dual interaction of ADP ribosylation factor 1 with Sec7 domain and with lipid membranes during catalysis of guanine nucleotide exchange, *J. Biol. Chem.* 274 (53) (1999) 37629–37636.

- [8] B. Antonny, S. Beraud-Dufour, P. Chardin, M. Chabre, N-terminal hydrophobic residues of the G-protein ADP-ribosylation factor-1 insert into membrane phospholipids upon GDP to GTP exchange, *Biochemistry* 36 (15) (1997) 4675–4684.
- [9] A. Spang, ARF1 regulatory factors and COPI vesicle formation, *Curr. Opin. Cell Biol.* 14 (2002) 423–427.
- [10] M. Franco, P. Chardin, M. Chabre, S. Paris, Myristoylation is not required for GTP-dependent binding of ADP-ribosylation factor ARF1 to phospholipids, *J. Biol. Chem.* 268 (3) (1993) 24531–24534.
- [11] A. Fensome, E. Cunningham, S. Prosser, S.K. Tan, P. Swigart, G. Thomas, J. Hsuan, S. Cockcroft, ARF and P1TP restore GTP $\gamma$ S-stimulated protein secretion from cytosol-depleted HL60 cells by promoting PIP<sub>2</sub> synthesis, *J. Biol. Chem.* 268 (3) (1993) 24531–24534.
- [12] R.A. Kahn, P. Randazzo, T. Serafiniga, O. Weiss, C. Rulka, J. Clark, M. Amherdt, P. Roller, L. Orci, J.E. Rothmann, The amino terminus of ADP-ribosylation factor (ARF) is a critical determinant of ARF activities and is a potent and specific inhibitor of protein transport, *J. Biol. Chem.* 267 (18) (1992) 13039–13046.
- [13] D.H. Jones, B. Bax, A. Fensome, S. Cockcroft, ADP ribosylation factor 1 mutants identify a phospholipase D effector region and reveal that phospholipase D participates in lysosomal secretion but is not sufficient for recruitment of coatamer 1, *Biochem. J.* 341 (1999) 185–192.
- [14] J. Goldberg, Structural and functional analysis of the ARF1-ARFGAP complex reveals a role for coatamer in GTP hydrolysis, *Cell* 96 (1999) 893–902.
- [15] M.G. Roth, Snapshots of ARF1: implications for mechanisms of activation and inactivation, *Cell* 97 (1999) 149–152.
- [16] J. Goldberg, Structural basis for activation of ARF GTPase: mechanisms of guanine nucleotide exchange and GTPMyristoyl switching, *Cell* 95 (1998) 237–248.
- [17] S.M.A. Davies, T.A. Harroun, T. Hauss, S.M. Kelly, J.P. Bradshaw, The membrane bound N-terminal domain of human adenosine diphosphate ribosylation factor-1 (ARF1), *FEBS Lett.* 548 (2003) 119–124.
- [18] K. Balali-Mood, T.A. Harroun, J.P. Bradshaw, Molecular dynamics simulations of a mixed DOPC/DOPG bilayer, *Eur. Phys. J., E Soft Matter* 12 (S01) (2003) S140–S135.
- [19] K. Balali-Mood, T.A. Harroun, J.P. Bradshaw, Membrane protein simulations using experimentally determined initial conditions, submitted for publication.
- [20] J.A. Losonczi, J.H. Prestegard, Nuclear magnetic resonance characterization of the myristoylated, N-terminal fragment of ADP-ribosylation factor 1 in a magnetically oriented membrane array, *Biochemistry* 37 (1998) 706–716.
- [21] J.A. Losonczi, F. Tian, J.H. Prestegard, Nuclear magnetic resonance studies of the N-terminal fragment of adenosine diphosphate ribosylation factor 1 in micelles and bicelles: influence of N-Myristoylation, *Biochemistry* 39 (2000) 3804–3816.
- [22] M.C. Weiner, S.H. White, Fluid bilayer structure determination by the combined use of X-ray and neutron diffraction: II. “Composition-space” refinement method, *Biophys. J.* 69 (1991) 174–185.
- [23] J.P. Bradshaw, M.J.M. Darkes, T.A. Harroun, J. Katsaras, R.M. Epand, Oblique membrane insertion of viral fusion peptide probed by neutron diffraction, *Biochemistry* 39 (22) (2000) 6581–6585.
- [24] M.C. Weiner, S.H. White, Fluid bilayer structure determination by the combined use of X-ray and neutron diffraction: I. Fluid bilayer models and the limits of resolution, *Biophys. J.* 69 (1991) 162–173.
- [25] R. Brasseur, Tilted peptides: a motif for membrane destabilization (Hypothesis), *Mol. Membr. Biol.* 17 (2000) 31–40.
- [26] P.J. Kraulis, MOLSCRIPT: a program to produce both detailed and schematic plots of protein structures, *J. Appl. Crystallogr.* 24 (1992) 946–950.